

Escape of photons from two fixed extreme Reissner-Nordström black holes

Daniel Alonso, Antonia Ruiz and Manuel Sánchez-Hernández

Departamento de Física Fundamental y Experimental,

Electrónica y Sistemas.

Universidad de La Laguna,

La Laguna 38203, Tenerife, Spain

We study the scattering of light (null geodesics) by two fixed extreme Reissner-Nordström black holes, in which the gravitational attraction of their masses is exactly balanced with the electrostatic repulsion of their charges, allowing a static spacetime. We identify the set of unstable periodic orbits that constitute the fractal repeller that completely describes the chaotic escape dynamics of photons. In the framework of periodic orbit theory, the analysis of the linear stability of the unstable periodic orbits is used to obtain the main quantities of chaos that characterize the escape dynamics of the photons scattered by the black holes. In particular, the escape rate which is compared with the result obtained from numerical simulations that consider statistical ensembles of photons. We also analyze the dynamics of photons in the proximity of a perturbed black hole and give an analytical estimation for the escape rate in this system.

PACS numbers: 05.45.-a, 04.70.Bw

I. INTRODUCTION

In general relativity, the nonexistence of an absolute time parameter introduces new aspects in the characterization of chaos with respect to the well-known Newtonian dynamics [1]. Some relativistic systems in which the existence of chaos has been reported include charged particles in a magnetic field interacting with gravitational waves, spinning particles orbiting rotating and nonrotating black holes, gravitational waves from spinning compact binaries, as well as particles in Majumdar-Papapetrou geometries.

Most of the studies of chaos around black holes have focussed on the analysis of the qualitative changes in the dynamics of an isolated black-hole spacetime caused by a small perturbation due to external mass distributions [2, 3, 4, 5], gravitational waves [6], spin-orbit and spin-spin coupling [7], or magnetic fields [8]. Recently, the projects to startup operative ground-base gravitational wave detectors (LIGO, VIRGO, GEO600, TAMA300, AIGO) and a planned laser interferometer space

antenna (LISA) [9], which will be able to detect the signals from gravitational wave sources, such as inspiralling compact binary systems of neutron stars or black holes, have increased the interest in the presence of chaos in the dynamics of binary black holes and its effects on the outgoing gravitational radiation [10].

In this work we use the Majumdar-Papapetrou metric [11] to analyze the dynamics of photons in the gravitational field of two extreme Reissner-Nordström black holes that are fixed in space due to the balance of their gravitational attraction and electrostatic repulsion. Although it is unlikely that this metric describes any astrophysical system, since in real universe black holes tend to rotate around their center of mass producing gravitational waves and do not possess overall electric charge, the chaotic scattering of photons in the Majumdar-Papapetrou static spacetime of nonrotating black holes with extreme electric charge still provides an interesting formal model that can be used to illustrate many of the features expected in more realistic systems.

In [2] Chandrasekhar studied the scattering of radiation by two extreme Reissner-Nordström black-holes that are at finite distance apart. In contrast to the two center problem in Newtonian gravitation, in general relativity this two center gravitational problem is generally not integrable. An appendix in [2] displays a set of null geodesics (photon's trajectories) in the meridian plane of the system and the conclusion was that probably the problem is not separable.

Shortly after, Contopoulos [3] systematically studied the set of photon trajectories with zero angular momentum component along the axis that goes through the black-holes. In that case the motion is confined to a plane (the meridian plane). The main conclusions of the study were that there are three types of non periodic motions. There are orbits that fall into one of the black-holes, with mass M_1 or mass M_2 , these are orbits of type *I* and *II*, and there are orbits that escape to infinity, these are orbits of type *III*. The orbits of different types are separated by orbits that tend asymptotically to three main types of unstable periodic orbits. One kind of periodic orbits goes around one of the black-holes, either M_1 or M_2 . A third type of unstable periodic orbits goes around the two black-holes. Between two non periodic orbits of two different types there are orbits of a third type. In this system chaos appears explicitly in the fact that the initial conditions of these types of orbits form a Cantor set. Further numerical evidence was given in favor that all periodic orbits for photons are unstable. In the same direction it was investigated the phase space trajectories in a multi-black-hole spacetimes [4] and found that the chaotic geodesics were well described by Lyapunov exponents. All these works give a strong indication that the scattering of photons by two Reissner-Nordström black-holes held fixed is chaotic and that the set of periodic orbits is unstable. The chaotic behavior of the relativistic null-geodesic motion on the two black

hole spacetime was also demonstrated by the geometric analysis of the flow [12]. More recently Contopoulos *et al.* have studied in detail the asymptotic curves from the periodic orbits, their homoclinic and heteroclinic intersections and the basins of attraction of two black holes [13].

It turns out that if a set of photons is launched against the black-holes, some of them will be trapped within the black-holes and others will escape to infinity. The escape dynamics of photons is closely related to the set of unstable periodic orbits of the system [14, 15, 16] and they describe such dynamics in a precise way. This set of periodic orbits forms a fractal set called the *repeller* which has a non integer Hausdorff dimension, and is characterized by the information dimension. The degree of dynamical randomness present in the system is measured by the Kolmogorov-Sinai entropy that has units of digits per second. The Kolmogorov-Sinai entropy can also be obtained from the set of unstable periodic orbits.

Our aim is to give a full description of the chaotic escape dynamics of photons in the two black-hole system in terms of the above mentioned quantities. We shall analyze the linear stability of the dynamics, in particular the unstable periodic orbits, and with that information evaluate the escape rate associated with the equations of motion using the well known trace formula for hyperbolic flows of Cvitanovic and Eckhardt [15]. It turns out that the escape rate is given by the leading eigenvalue of the spectrum of the evolution operator [16]. In addition, we shall compare our results with numerical simulations that consider the evolution with time of statistical ensembles of photons.

In Section II we give a summary of Chandrasekhar's model to describe the dynamics of photons under the gravitational field of two extreme Reissner-Nordström black holes. In Section III we discuss the linear stability of the dynamics and the general methods that we will consider to obtain the escape dynamics of photons. Section IV introduces the formalism to study the time evolution of statistical ensembles of photons and their escape dynamics. In Section V we present the set of periodic orbits of the system in the meridian plane ($L_z = 0$) and give their periods and stretching factors. In Section VI we calculate the main quantities of chaos derived from the analysis of the linear stability of the unstable periodic orbits. The escape rate obtained from the periodic orbit theory is compared with value obtained from numerical simulations that consider statistical ensembles of photons. In Section VII we analyze the dynamics in the proximity of a perturbed black hole and give an analytical estimation for the escape rate in this system. In Section VIII the main conclusions are put together.

II. DYNAMICAL EQUATIONS

The model studied by Chandrasekhar in [2] comes from the solutions of the Einstein-Maxwell equations which describe a problem analogous to the Newtonian arrangement of charged mass-points where the mutual Coulomb repulsions are balanced by the gravitational attraction. These solutions are known as Majumdar-Papapetrou solutions [11]. They are obtained from an static solution of the Einstein-Maxwell equations [17]. The metric of the Majumdar-Papapetrou solution of the Einstein-Maxwell equations is given by

$$ds^2 = dt^2/U^2 - U^2(dx^2 + dy^2 + dz^2), \quad (1)$$

where (x, y, z) are the spatial coordinates. The function U , which depends only on the spatial coordinates, is a solution of the three-dimensional Laplace's equation

$$\nabla^2 U = \left(\frac{\partial^2}{\partial x^2} + \frac{\partial^2}{\partial y^2} + \frac{\partial^2}{\partial z^2} \right) U = 0. \quad (2)$$

Hartle and Hawking [18] gave the interpretation of the Majumdar-Papapetrou solution; they showed that for a function U of the form

$$U = 1 + \sum_{i=1}^N \frac{M_i}{r_i}, \quad (3)$$

where $r_i = \sqrt{(x - x_i)^2 + (y - y_i)^2 + (z - z_i)^2}$, this solution corresponds to a system of N extreme Reissner-Nordström black holes with horizons at (x_i, y_i, z_i) and with masses equal to their charges, $M_i = Q_i > 0$. The metric is everywhere regular except at the locations of the black-holes where there are coordinate singularities, as argued in [2, 17].

We will consider a configuration of two black holes located at $z = \pm z_{bh}$, lying on the z -axis. Using geometrized units (the speed of light in vacuum $c = 1$ and the gravitational constant $G = 1$) the function U takes the form

$$U = 1 + \frac{M_1}{(x^2 + y^2 + (z - z_{bh})^2)^{1/2}} + \frac{M_2}{(x^2 + y^2 + (z + z_{bh})^2)^{1/2}}. \quad (4)$$

The Lagrangian \mathcal{L} associated with the metric (1) is defined by

$$\mathcal{L} = \frac{\dot{t}^2}{2U^2} - \frac{U^2}{2}(\dot{x}^2 + \dot{y}^2 + \dot{z}^2), \quad (5)$$

where the dot denotes the derivative with respect to the affine parameter. From this Lagrangian the following Hamiltonian \mathcal{H} can be derived

$$\mathcal{H} = -\frac{1}{2}U^2 p_t^2 + \frac{1}{2}U^{-2}(p_x^2 + p_y^2 + p_z^2). \quad (6)$$

Thus the Hamilton's equations that govern the geodesic motion in the space-time with the metric (1) are

$$\begin{aligned} \dot{x} &= U^{-2}p_x, & \dot{p}_x &= \frac{1}{2}\partial_x(U^2 - U^{-2}P^2) \\ \dot{y} &= U^{-2}p_y, & \dot{p}_y &= \frac{1}{2}\partial_y(U^2 - U^{-2}P^2) \\ \dot{z} &= U^{-2}p_z, & \dot{p}_z &= \frac{1}{2}\partial_z(U^2 - U^{-2}P^2). \end{aligned} \quad (7)$$

It follows from the Hamilton's equations that $p_t = E = \text{constant}$ and that $L_z = xp_y - yp_x = \text{constant}$, which is the angular momentum along the z -axis. In the case of photons it follows also that $\mathcal{H} = -U^2E^2/2 + U^{-2}(p_x^2 + p_y^2 + p_z^2)/2 = 0$ [2, 3], and therefore $p_x^2 + p_y^2 + p_z^2 = P^2 = U^4E^2$. Hence the problem scales with E and without loss of generality we can consider $E = 1$.

Due to the conservation of L_z the motion for $L_z = 0$ is restricted to a plane (meridian plane). We shall take this simplification and study the motion in the meridian plane.

III. LINEAR STABILITY

We are particularly interested in the analysis of the stability of the solutions of the equations of motion, i.e. how is their behavior when they are slightly perturbed. To fix the notation and make the paper self contained, in this section we introduce the basic concepts of linear stability. First we shall discuss this problem in a general context. Then the application to the two black holes system is straightforward.

Let us consider a Hamiltonian system with f degrees of freedom. The $2f$ -dimensional phase-space can be denoted by $X = (X_1, X_2, \dots, X_{2f})$, where the first f -components of X are the generalized coordinates and the rest of the components are the generalized momenta. If we denote by Σ a $2f \times 2f$ antisymmetric matrix of the symplectic form

$$\Sigma = \begin{pmatrix} 0 & 1 \\ -1 & 0 \end{pmatrix}, \quad (8)$$

with 0 and 1 the $f \times f$ null and unit matrices respectively. The Hamilton's equations for a Hamiltonian \mathcal{H} can be expressed as

$$\dot{X} = \Sigma \cdot \frac{\partial \mathcal{H}}{\partial X}. \quad (9)$$

A solution X_s of these differential equations is a curve in phase-space with some initial condition X_0 . The analysis of the stability of this solution involves the study of the evolution with time of a

small perturbation δX with respect to X_s . Considering $Y_s = X_s + \delta X$, it follows that δX satisfies the initial value problem

$$\delta \dot{X} = \mathbf{L}(s) \cdot \delta X, \quad (10)$$

with $\mathbf{L}(s) = \Sigma \cdot \frac{\partial^2 \mathcal{H}}{\partial X^2}|_{X_s}$. This is a linear initial value problem with time-dependent coefficients. For an initial perturbation δX_0 it has the solution

$$\delta X_s = \mathbf{M}(s) \cdot \delta X_0. \quad (11)$$

The $2f \times 2f$ matrix \mathbf{M} is usually referred as the *fundamental matrix* and gives the time evolution of an initial displacement δX_0 . The fundamental matrix is, by itself, a solution of the differential equation

$$\dot{\mathbf{M}} = \mathbf{L}(s) \cdot \mathbf{M}, \text{ with } \mathbf{M}(0) = 1. \quad (12)$$

The behavior of the perturbation δX can be analyzed in terms of the Lyapunov exponents of X_s , which measure the rate of exponential separation or approach of initially infinitely close trajectories. The Lyapunov exponent associated with the unit vector $\mathbf{e}_j = \delta X_j / |\delta X_j|$ in the direction of δX_j is given by

$$\lambda(X_0, \mathbf{e}_j) = \lim_{s \rightarrow \infty} \frac{1}{s} \ln |\mathbf{M}(X_0, s) \cdot \mathbf{e}_j|. \quad (13)$$

The number of Lyapunov exponents equals the dimension of phase-space. Positive Lyapunov exponents are evidence for dynamical instability of trajectories in phase space, and therefore an extreme sensitivity to the initial conditions.

For a periodic orbit X_s , the Lyapunov exponents are directly related to the stability of this solution. The Lyapunov exponents can be degenerate with multiplicity m_i , in the sense that several of them have the same value. They are ordered as $\lambda_1 \geq \lambda_2 \geq \dots \geq \lambda_\nu$ with $\sum_{i=1}^{\nu} m_i = 2f$. The fundamental matrix has a symplectic structure and therefore satisfies the relation $\mathbf{M}^T \Sigma \mathbf{M} = \Sigma$ [19]. Due to this property all the Lyapunov exponents in Hamiltonian systems are grouped in pairs of equal absolute value and opposite sign $\{\lambda_i, -\lambda_i\}_{i=1, \dots, f}$. Furthermore, perturbations along the direction of the flow give a zero Lyapunov exponent, and due to the pairing property another one is also zero, which is a consequence of the conservation of energy [20, 21]. Thus at least two exponents are zero.

As we mentioned before the periodic orbits are a distinguished set of solutions. For these solutions the matrix $\mathbf{M}(s)$ is also periodic with the same period. In general $X_s = X_{s+T}$, with

$T = rT_p$ ($r=1,2,\dots$) and T_p the primitive period of the orbit. The linear stability of a periodic orbit is given by the eigenvalues of $M(s)$ over one primitive period, i.e. $M(T_p)$. Such eigenvalues are obtained from the secular determinant

$$\det [M(T_p) - \Lambda 1] = 0. \quad (14)$$

Due to the symplectic property of the fundamental matrix its eigenvalues Λ_j , called *stretching factors* or *stability eigenvalues*, are also grouped in pairs. From the previous discussion two of them are equal to one. One of them corresponds to perturbations along the periodic orbit and the other to perturbations perpendicular to the energy shell. The Lyapunov exponents associated with a periodic orbit are given in terms of the stretching factors as $\lambda_i = \ln |\Lambda_i|/T_p$.

The stability of a particular motion is determined by the location of the stretching factor in the complex plane. $|\Lambda_i| > 1$ is a signature of instability and corresponds to the unstable manifold of the periodic orbit. The stability eigenvalues such that $|\Lambda_i| < 1$ are related to the stable manifold and those with $|\Lambda_i| = 1$ correspond to the center manifold of the orbit.

A straightforward application, which is directly related to our problem, is the study of the dynamics of systems with two degrees of freedom. In such systems we say that the periodic orbit is *hyperbolic* when $\Lambda > 1 > \Lambda^{-1} > 0$. A periodic orbit is called *hyperbolic with reflection* when $\Lambda < -1 < \Lambda^{-1} < 0$. Finally the periodic orbit with $|\Lambda| = 1$ is called *elliptic* [19]. When Λ crosses the unit circle the periodic orbit changes its stability and, generally undergoes a bifurcation where some periodic orbits may disappear and others emerge. In autonomous systems the energy is the main bifurcation parameter. As we mentioned previously the dynamics of the photons in our system scales with energy so no bifurcation is expected.

It is clear that a periodic orbit is characterized by its primitive period and its stretching factors Λ_i . We shall see below how this information can be used to make a detailed analysis of the escape dynamics of photons scattered by two black-holes.

IV. EVOLUTION OF DENSITY OF PHOTONS AND THEIR DECAY DYNAMICS

The motion of a single photon in the meridian plane is chaotic and it is useful, in order to characterize its escape dynamics from the black-holes, to consider statistical ensembles that provide a probabilistic description of the process. Therefore, instead of analyzing a unique photon and its orbit, we consider an ensemble of them represented by some density ρ . For a given Hamiltonian \mathcal{H}

the evolution with time of a density ρ is given by the Liouville equation

$$\partial_s \rho = \hat{L} \rho, \quad (15)$$

with the Liouville operator \hat{L} given by the Poisson bracket as $\hat{L} = \{\mathcal{H}, \rho\}$. The Liouville equation is linear and for an initial density ρ_0 has as solution

$$\rho_s = e^{\hat{L}s} \rho_0, \quad (16)$$

for time-independent Hamiltonians. From (16), the average over the ensemble at time s of any observable A defined in the phase space of the system can be computed as;

$$\langle A \rangle_s = \int dX A(\Phi^s X) \rho_0(X), \quad (17)$$

where we have introduced the flow Φ^s , which maps an initial condition X_0 into X_s , as $X_s = \Phi^s X_0$. An alternative manner of writing this last equation is [20, 21]

$$\langle A \rangle_s = \int dX dY A(X) \delta(X - \Phi^s Y) \rho_0(Y), \quad (18)$$

where the Dirac distribution $\delta(X - \Phi^s Y)$ can be considered as the conditional probability density for the trajectory to be located at the point X by the time s if it was initially at the point Y . Indeed the Dirac distribution defines the kernel of the evolution operator. The equation (18) defines two operators which are adjoint of each other as

$$\langle A \rangle_s = \langle \hat{P}^{\dagger s} A | \rho_0 \rangle = \langle A | \hat{P}^s \rho_0 \rangle. \quad (19)$$

The evolution of a probability density is ruled by the *Frobenius-Perron* equation [20, 21]

$$\rho_s(X) = \hat{P}^s \rho_0(X) \equiv \int dY \delta(X - \Phi^s Y) \rho_0(Y) \quad (20)$$

while the time evolution of the observables is ruled by the Koopman operator [22] defined by

$$A_s(Y) = \hat{P}^{\dagger s} A(Y) \equiv \int dX \delta(X - \Phi^s Y) A(X). \quad (21)$$

If the flow Φ^s is invertible and conservative the Frobenius-Perron operator reduces to $\rho_s(X) = \hat{P}^s \rho_0(X) = \rho_0(\Phi^{-s} X)$. In open systems the trajectories that are initially confined in a bounded region in phase space tend to go to infinity with an exponential escape rate. For these systems, the number of particles $N(s)$ that remain inside the initial domain at instant s decays exponentially with time as $N(s) \sim N(0)e^{-\gamma s}$, where γ is the so called *escape rate*.

As a matter of fact, the leading eigenvalue of \hat{P}^s dominates the decay and determines the escape rate. The rest of the spectrum (*resonances*) describes further details of the dynamics and gives other important time scales beside the associated with the escape rate. Thus the spectrum of the Frobenius-Perron operator \hat{P}^s provides a way to describe the evolution of a set of trajectories characterized by a density $\rho_s(X)$. This spectrum gives enough information about the characteristic times of the decay, in particular about the escape dynamics from the system of interest.

The spectral theory of \hat{P}^s goes to back Koopman [22] and von Neumann [23]. It assumes that the evolution operator acts in a functional space of square integrable densities \mathcal{L}^2 . In such case the evolution is unitary and the eigenvalues of \hat{P}^s belong to the unit circle. The spectrum of a chaotic system presents continuous components in the unit circle which describe the decay of correlations functions for these systems. New methods [24, 25] have been developed to obtain eigenvalues of \hat{P}^s outside the unit circle and analyze the escape process or relaxation dynamics. These methods, which are valid for systems where all the periodic orbits are unstable, have been successfully used in chaotic systems and the study of transport phenomena among other applications [20, 21, 27, 28, 29]. We shall apply them to the study of the escape dynamics of photons from the two black holes.

One of the methods developed to obtain the spectrum computes the trace of the Frobenius-Perron operator. Here we shall outline this procedure and refer the reader to the specialized literature on the subject [20, 21, 24, 25, 26] for further details.

The trace of \hat{P}^s can be formally written as

$$Tr \hat{P}^s = \int dX \delta(X - \Phi^s X). \quad (22)$$

The contributions to the trace come from the fixed points of the flow, which are given by the condition

$$X = \Phi^s X, \quad (23)$$

for some s . In general this equation has two types of solutions. There are *stationary points* that satisfy (23) for all s , and there are *periodic orbits* which satisfy the fix-point condition for a discrete set of values of s , given by $s = rT_p$, with $r = 1, 2, \dots$. We assume that the solutions of (23) are isolated, which means that each stationary point or periodic orbit is locally unique. A periodic orbit may belong to a continuous family if there exists some continuous symmetry or some constant of motion. When this occurs the domain of integration in (22) has to be reduced into a smaller one with less dimensions, until the periodic orbit is completely isolated. In time-independent Hamiltonian systems the periodic orbits are rarely isolated, instead they tend to form continuous

families when the energy changes. Therefore the phase-space has to be reduced using the energy conservation $\mathcal{H} = E$. Then the trace (22) is formally given by

$$Tr_E \hat{P}^s = \int_E d^{2f-1}x \delta(X - \phi_E^s x), \quad (24)$$

where ϕ_E^s denotes the flow on the energy shell [15, 20]. If any additional symmetry is present in the system then further reductions are required. Here we are considering the dynamics on the energy shell and we have removed the axial symmetry by choosing a particular meridian plane. Hence all the periodic orbits of the flow in our system can be treated as isolated.

The trace (24) can be written in terms of the unstable periodic orbits of the flow [14, 15] and their repetitions. To do so the integral in (24) must be done using a set of coordinates such that one of them is parallel to the periodic orbit and the remaining coordinates are transversal to it. We remind we are assuming that all the periodic orbits are isolated. The integral over the coordinate along the orbit is trivial and it is related to the period of the orbit. On the other hand, the integration over the transversal coordinates takes into account the stability of the periodic orbit. The result for the trace is [15]

$$Tr \hat{P}^s = \sum_{p=p.p.o.} \sum_{r=1}^{\infty} T_p \frac{\delta(s - rT_p)}{|\det(1 - \mathbf{m}_p^r)|} \quad (s > 0), \quad (25)$$

where the sums are over *primitive periodic orbits* (*p.p.o.*) and their r repetitions. The matrix \mathbf{m}_p is derived from the fundamental matrix $\mathbf{M}(T_p)$ once the perturbations along the orbit and the perturbations perpendicular to the energy shell have been removed. Hence in a two-dimensional flow the matrix \mathbf{m}_p contains only the stretching factors whose modulus is different from one. These are precisely the ones related to the stable and unstable manifolds of the isolated unstable periodic orbit.

Formally the Laplace transform of the Frobenius-Perron operator gives the resolvent of the Liouville operator defined in (15), which using (24) can be written as

$$Tr \frac{1}{\sigma - \hat{L}} = \int_0^{\infty} ds e^{-\sigma s} Tr \hat{P} = \frac{\partial}{\partial \sigma} \ln Z(\sigma), \quad (26)$$

where $Z(\sigma)$ is the so called Selberg-Smale Zeta function [30] given by

$$Z(\sigma) \equiv \exp \left(- \sum_{p=p.p.o.} \sum_{r=1}^{\infty} \frac{1}{r} \frac{e^{-\sigma r T_p}}{|\det(1 - \mathbf{m}_p^r)|} \right) \quad (27)$$

If we denote by Λ_p and Λ_p^{-1} the eigenvalues of \mathbf{m}_p , the zeta function can be expressed as

$$Z(\sigma) = \prod_{p=p.p.o.} \prod_{k=0}^{\infty} \left(1 - \frac{e^{-\sigma T_p}}{|\Lambda_p| \Lambda_p^k} \right)^{k+1}. \quad (28)$$

where $\Lambda_p > 1$ since in the two black-hole system all the periodic orbits are unstable. It follows from the derivation that the zeroes of function $Z(\sigma)$ give the spectrum of the system. Such function is usually expressed as the product of the inverse of *Ruelle* ζ -functions as

$$Z(\sigma) = \zeta_0^{-1}(\sigma) \zeta_1^{-2}(\sigma) \zeta_2^{-3}(\sigma) \cdots \quad (29)$$

with the definition

$$\zeta_k^{-1}(\sigma) = \prod_{p=p.p.o} \left(1 - \frac{e^{-\sigma T_p}}{|\Lambda_p| \Lambda_p^k} \right). \quad (30)$$

The relaxation times τ_i associated with the dynamics are given by the poles of the resolvent of the Liouvillian, as $Re \sigma_i = \tau_i^{-1}$, or equivalently, from the zeroes of the zeta function or the zeroes of the inverse of the Ruelle ζ -functions. The leading part of the spectrum is given by the poles of the first Ruelle ζ -function $\zeta_0(\sigma)$ (or zeroes of ζ_0^{-1}). So we are mainly interested in the part of the spectrum that controls the long-time behavior of the dynamics.

The set of unstable periodic orbits can be used to describe in fine detail the escape dynamics of photons from the black holes. This set forms a fractal set called the *repeller*. The number of periodic orbits in such set grows exponentially with the period, with a rate of the proliferation that is given by the topological entropy h_{top} . The amount of chaos in the system is given by the Kolmogorov-Sinai entropy per unit time h_{KS} , which measures the minimal data accumulation rate required to reconstruct a trajectory on the repeller without ambiguity. The repeller has a mean Lyapunov exponent λ . In a Poincare section that is transverse to the flow on the repeller, the fractal repeller defines another fractal which is characterized by the partial generalized fractal dimensions. Two representative partial dimensions are the Hausdorff dimension d_H , which characterizes the bulkiness of the repeller in phase space, and partial information dimension d_I that can be obtained from the Kolmogorov-Sinai entropy and the mean Lyapunov exponent as $d_I = h_{KS}/\lambda$ [16].

The different quantities that characterize the repeller can be obtained from the so called topological pressure $P(\beta)$ [31], which can be determined from the periodic orbits of the repeller as the leading zero of a Ruelle ζ -function

$$\zeta_\beta^{-1}(\sigma) \equiv \prod_{p=p.p.o} \left(1 - \frac{e^{-\sigma T_p}}{|\Lambda_p|^\beta} \right). \quad (31)$$

The mean Lyapunov exponent for trajectories on the fractal repeller is $\lambda = -dP(1)/d\beta$, the escape rate is $\gamma = -P(1)$ and the topological entropy is given by $h_{top} = P(0)$. In Hamiltonian systems with two degrees of freedom the Kolmogorov-Sinai entropy follows from $h_{KS} = \lambda - \gamma$ [32]. The partial Hausdorff dimension is obtained from $P(d_H) = 0$ and the information dimension is given by $d_I = 1 - \gamma/\lambda$.

V. PERIODIC ORBITS IN THE MERIDIAN PLANE ($L_z = 0$)

From now on we shall focus on the analysis of the escape dynamics of photons from the black holes in the meridian plane. As we have just mentioned, there are some important objects that can be used to describe this dynamics. First we need to identify the set of periodic orbits and their corresponding primitive periods. To analyze the linear stability of each unstable periodic orbit we must integrate in time its fundamental matrix up to one primitive period. The eigenvalues of the resulting matrix give the stretching factors associated with the orbit. Then, once we know the periods and the stretching factors of the unstable periodic orbits, the main quantities of chaos that characterize the dynamics can be obtained following the methods introduced in the previous section.

The restriction on the motion to the meridian plane $L_z = 0$ simplifies the set of equations to be integrated. Without loss of generality we can consider that the photons move in the (x, z) -plane. Then the equations of motion (7) reduce to

$$\begin{aligned} \dot{x} &= U^{-2}p_x, & \dot{p}_x &= \frac{1}{2}\partial_x(U^2 - U^{-2}P^2) \\ \dot{z} &= U^{-2}p_z, & \dot{p}_z &= \frac{1}{2}\partial_z(U^2 - U^{-2}P^2). \end{aligned} \quad (32)$$

These equations were integrated using a Runge-Kutta-Fehlberg method, and the search for periodic orbits was performed using the Newton-Raphson method.

The periodic orbits in the system can be classified according to a symbolic coding. Taking as reference the symmetry axis that contains the two black holes, in our system of coordinates the z -axis, we introduce a series of symbols to label these orbits. An orbit can cross the z -axis either above the black-hole located at $z = z_{bh}$, below the black-hole located at $z = -z_{bh}$ or in between the two black-holes. We label each crossing that occurs at $z > z_{bh}$ with the symbol “+”; to indicate a crossing at $z < -z_{bh}$ we use the symbol “−”. When an orbit crosses the z -axis twice at the same point in between the two black holes, drawing an “×” on the axis, we use the symbol “o”. Any other crossing in between the two black holes is indicated with the symbol “+” or the symbol “−” depending on the sign of the coordinate z at the crossing point, $z > 0$ (+) or $z < 0$ (−). Figure (1) displays the set of unstable periodic orbits numerically found and their corresponding symbolic coding. The primitive period of each orbit is given in Table (I).

To compute the stretching factors of the set of unstable periodic orbits, each orbit was numerically integrated together with its corresponding fundamental matrix up to one primitive period of the orbit. In order to obtain the stability factors with certain precision it is important to compute

Symbolic coding	Period T_p	Stretching factor Λ_p
$\{++\}, \{--\}$	4.1180374	99.1244899
$\{+-\}$	15.292055	215.721472
$\{+ \circ - \circ\}$	10.608412	16996.3144
$\{+ - ++\}, \{- + --\}$	18.900782	30044.8517
$\{+++ \circ - \circ\}, \{- - - \circ + \circ\}$	14.739760	1.70990814×10^6
$\{++++ --\}$	22.635603	3.97082132×10^6
$\{+ - + \circ - \circ\}, \{- + - \circ + \circ\}$	25.410381	4.57097810×10^6
$\{+ - + + + -\}, \{- + - - - +\}$	34.185532	6.49738275×10^6
$\{+++ \circ - - - \circ\}$	18.871204	1.72085241×10^8
$\{+ - - - - + +\}, \{- + + + + - -\}$	26.748625	3.95770189×10^8
$\{+ - + \circ - - - \circ\}, \{- + - \circ + + + \circ\}$	29.542461	4.59225358×10^8
$\{+ - + \circ - - - \circ + -\}, \{- + - \circ + + + \circ - +\}$	44.828729	$9.92347816 \times 10^{10}$

TABLE I: The periods and stretching factors of the unstable periodic orbits depicted in figure (1).

the unstable periodic orbit with high accuracy. In Table (I) are listed the non-trivial stretching factors of the periodic orbits. We recall that these are the stretching factors that are related to the transversal directions to the periodic orbit.

As the values in the Table (I) indicate, the trajectories $\{++\}(\{--\})$, $\{+-\}$ and $\{+ \circ - +\}$ have the lowest stability eigenvalues. The rest of the orbits are much more unstable as they have larger stretching factors. In general the more stable periodic orbits should dominate the asymptotic escape of particles from the two black-hole configuration.

VI. ESCAPE RATE IN THE MERIDIAN PLANE AND OTHER CHARACTERISTIC QUANTITIES OF CHAOS

With the primitive periods T_p and stretching factors Λ_p of the set of unstable periodic orbits we can compute, following the methods described in Section IV, the escape rate of the system as well as other characteristic quantities of the dynamics related to the fractal repeller of the unstable periodic orbits. To this aim we consider the cycle expansion method [14, 15] which has been successfully applied to other hyperbolic systems [27]. Due to the high instability of higher order periodic orbits (longer symbolic coding) only three main periodic orbits, $\{++\}(\{--\})$, $\{+-\}$ and $\{+ \circ - +\}$, contribute significantly to the escape rate. Indeed they give an acceptable escape rate and the different quantities of chaos.

λ	γ	h_{KS}	h_{top}	d_H	d_I
0.388	0.340	0.048	0.167	0.288	0.124

TABLE II: Characteristic quantities of chaos related to the fractal repeller of the unstable periodic orbits given in figure (1). λ is the mean Lyapunov exponent of the repeller, γ the escape rate, h_{KS} the Kolmogorov-Sinai entropy, h_{top} the topological entropy, d_H the Hausdorff dimension and d_I the partial information dimension.

Figure (2) shows the pressure function obtained from these three periodic orbits. The main quantities of chaos obtained from this pressure function and its derivative are listed in Table (II).

In particular, the escape rate which takes a numerical value $\gamma = 0.340$. From the analysis of the linear stability of the set of unstable periodic orbits, it could be assumed that the escape dynamics of photons from the two black holes is mainly controlled by the outermost periodic orbit $\{+-\}$. If only such orbit is considered it follows an escape rate

$$\gamma_{+-} = \frac{\ln |\Lambda_{+-}|}{T_{+-}} = 0.351, \quad (33)$$

which is quite close to the escape rate obtained from the pressure function. Thus, we can conclude that the orbit $\{+-\}$ dominates the effective escape of photons from the two black-hole configuration. A photon that crosses out this orbit escapes to infinity and does not come back to the proximity of the black holes.

In the following section we contrast the escape rate value derived from the analysis of the linear stability of the periodic orbits with the escape rate obtained from numerical simulations that consider the time evolution of large statistical ensembles of photons.

A. Numerical simulations with statistical ensembles

We consider an ensemble of photons with initial positions uniformly distributed along the z -axis and initial velocity parallel to the x -axis. This together with the energy conservation completely defines the ensemble. Once all initial conditions have been fixed the evolution with time of each photon of the ensemble is numerically integrated. Some of the photons fall into one of the two black holes, while others escape to infinity. We are precisely interested in the second subset of trajectories. To compute the escape rate we consider a circle of control that covers the two black holes and which is larger than the outermost periodic orbit $\{+-\}$. Hence we can be sure that all the photons that cross out this circle escape to infinity and never come back to the proximity of the black holes.

Let us denote by $N(t)$ the number of photons that remain inside the circle of control at time t (this includes the photons that fall into the black-holes). This function will decay in time until it reaches an asymptotic value $N(\infty)$, which gives the number of photons that fall into the black holes. The escape rate γ is defined by the exponential decay to zero of the function $[N(t) - N(\infty)]$ for long enough time; $[N(t) - N(\infty)] \approx [N(0) - N(\infty)]e^{-\gamma t}$ as $t \rightarrow \infty$.

Figure (3) shows the results obtained from different simulations that include an increasing number of particles in the statistical ensemble. As it can be seen, the larger is the number of particles of the ensemble the longer persists the exponential decay in time. From the slope of these curves we extract a numerical escape rate $\gamma_{num} = 0.344$. The agreement with the escape rate obtained from the analysis of the linear stability of the unstable periodic orbits, see Table (II), is excellent. This result confirms our expectation with respect to the subset of periodic orbits that plays the main role in the escape dynamics. The additional structure observed in the evolution of the function $[N(t) - N(\infty)]$ can be explained from the lower resonances of the system. This point has been emphasized in [27].

Clearly, the escape rate of photons depends on the masses of the black holes and the separation distance between them. The larger are the masses the more extended in space are the unstable periodic orbits of the fractal repeller that marks the boundary between dynamical stability and instability, and therefore the regions where the light rays fall into the black holes. It could be expected then that the escape rate of photons decreases as the masses of the black holes become larger. Figure (4) illustrates this behavior and shows the decay of the escape rate as the mass of one black hole increases and the other mass remains constant. As figure (5) shows, the escape rate can also decrease due to the enlargement of the region of trapping of photons by the black holes as the separation distance between them becomes larger.

In figure (5) we consider the scattering of photons from two black holes with masses $M_1 = M_2 = M$, located at different positions $(0, \pm d)$. From (4) and (7) it can be easily shown that a system of two black holes with scaled masses $\tilde{m}_1 = \tilde{m}_2 = M/d$ located at $(0, \pm 1)$ satisfies identical dynamics with respect to an scaled affine parameter η defined by $\dot{q} = dq/d\tau = d\tilde{q}/d\eta$ ($d\eta = d\tau/d$), being $\tilde{q} = q/d$ ($q = x, y, z$) scaled distances. Hence if we denote γ_d the escape rate from two identical black holes of mass M located at $(0, \pm d)$, and $\tilde{\gamma}$ the escape rate from two black holes of the same mass $\tilde{m} = M/d$ located at $(0, \pm 1)$, it follows that $\gamma_d = \tilde{\gamma}/d$.

VII. ESCAPE DYNAMICS OF PHOTONS FROM A PERTURBED BLACK HOLE

In this section we analyze the escape rate from an extreme Reissner-Nordström black hole of mass M_1 that is slightly perturbed by the interaction with an extreme Reissner-Nordström black hole of mass M_2 located at distance d . In polar coordinates, the Hamiltonian can be written as

$$\mathcal{H} = \frac{h}{U^2} = \frac{1}{U^2} \left[\frac{1}{2} \left(p_r^2 + \frac{p_\theta^2}{r^2} \right) - \frac{U^4}{2} \right] \quad (34)$$

with the function U given by:

$$U = 1 + \frac{M_1}{r} + \frac{M_2}{\sqrt{r^2 + d^2 - 2rd \sin \theta}} \quad (35)$$

The analysis of the dynamics can be greatly simplified introducing a scaling in the equations of motion

$$\dot{X} = \frac{dX}{d\tau} = \Sigma \cdot \frac{\partial \mathcal{H}}{\partial X} \quad X = (r, \theta, p_r, p_\theta) \quad (36)$$

in the form

$$X' = \frac{dX}{d\xi} = \Sigma \cdot \frac{\partial h}{\partial X} \quad X = (r, \theta, p_r, p_\theta) \quad (37)$$

with a *scaled* affine parameter ξ defined by $d\xi = d\tau/U^2$. In these new equations, the Hamiltonian h is just the kinetic energy term plus an interaction term $-U^4/2$. The function U^4 may be expressed as an expansion in powers of (d/r) , with the first two terms given by:

$$U^4 = \left(1 + \frac{M_1 + M_2}{r} \right)^4 + \frac{4M_2 d}{r^2} \left(1 + \frac{M_1 + M_2}{r} \right)^3 \sin \theta + \mathcal{O} \left[\left(\frac{d}{r} \right)^2 \right] \quad (38)$$

In the limit $(M_1 + M_2)^2 \gg 2M_2 d$ the dynamics of the system is dominated by the radial term in the expansion (38), which is perturbed by the remaining angular terms. Thus to zero order approximation the space time associated with the two extreme black holes becomes spherically symmetric. There exists a single unstable periodic orbit which is a circle of radius $r = M \equiv (M_1 + M_2)$ and period $T_\xi = M\pi/2$. The time evolution along this orbit is given by

$$\begin{aligned} r_s(\xi) &= M & \theta_s(\xi) &= \theta_0 + \frac{4}{M}\xi \\ p_{rs}(\xi) &= 0 & p_{\theta s}(\xi) &= L \end{aligned} \quad (39)$$

with angular momentum $L = 4M$. The periodic orbit associated with the Hamiltonian \mathcal{H} is also a circle of radius $r = M \equiv (M_1 + M_2)$, but with period $T = 2\pi M$. The time evolution along this orbit is given by: $r_s(\tau) = M$, $\theta_s(\tau) = \theta_0 + \tau/M$, $p_{rs}(\tau) = 0$ and $p_{\theta s}(\tau) = L$.

To zero order approximation the escape rate of photons from an *effective* black hole of mass M can be determined from the analysis of the linear stability of the circular orbit (39), $X_s \equiv (r_s, \theta_s, p_{rs}, p_{\theta s})$. This implies the study of the time evolution of a small perturbation, $\delta X \equiv (\delta r, \delta \theta, \delta p_r, \delta p_\theta)$, with respect X_s . Considering the scaled Hamiltonian h , the linear differential equations that describe such evolution, $\delta X' = l(s) \cdot \delta X$ with $l(s) = \Sigma \cdot \frac{\partial^2 h}{\partial X^2}|_{X_s}$, are:

$$\begin{pmatrix} \delta r' \\ \delta \theta' \\ \delta p_r' \\ \delta p_\theta' \end{pmatrix} = \begin{pmatrix} 0 & 0 & 1 & 0 \\ -\frac{8}{M^2} & 0 & 0 & \frac{1}{M^2} \\ \frac{8}{M^2} & 0 & 0 & \frac{8}{M^2} \\ 0 & 0 & 0 & 0 \end{pmatrix} \cdot \begin{pmatrix} \delta r \\ \delta \theta \\ \delta p_r \\ \delta p_\theta \end{pmatrix} \quad (40)$$

and the fundamental matrix $M(\xi)$, solution of $M' = l(s) \cdot M$ with $M(0) = 1$, is given by

$$M(\xi) = \begin{pmatrix} C(\xi) & 0 & \frac{M}{2\sqrt{2}}S(\xi) & [C(\xi) - 1] \\ -\frac{2\sqrt{2}}{M}S(\xi) & 1 & [1 - C(\xi)] & [\frac{9}{M^2}\xi - \frac{2\sqrt{2}}{M}S(\xi)] \\ \frac{2\sqrt{2}}{M}S(\xi) & 0 & C(\xi) & \frac{2\sqrt{2}}{M}S(\xi) \\ 0 & 0 & 0 & 1 \end{pmatrix} \quad (41)$$

with

$$C(\xi) = \cosh\left(\frac{2\sqrt{2}}{M}\xi\right) \quad \text{and} \quad S(\xi) = \sinh\left(\frac{2\sqrt{2}}{M}\xi\right) \quad (42)$$

The stretching factors associated with the circular orbit are obtained from the eigenvalues of the matrix $M(\xi)$,

$$\left\{1, 1, e^{-\frac{2\sqrt{2}}{M}\xi}, e^{\frac{2\sqrt{2}}{M}\xi}\right\}, \quad (43)$$

evaluated at one primitive period T_ξ . That is,

$$\Lambda = \left\{1, 1, e^{-\sqrt{2}\pi}, e^{\sqrt{2}\pi}\right\}. \quad (44)$$

As expected, two stretching factors are equal to one. The values $e^{-\sqrt{2}\pi}$ and $e^{\sqrt{2}\pi}$ are related to the stable and unstable manifolds of the unique unstable periodic orbit respectively. The Lyapunov exponents associated with this orbit are given by

$$\frac{\ln |\Lambda|}{T} = \left\{0, 0, -\frac{1}{\sqrt{2}M}, \frac{1}{\sqrt{2}M}\right\} \quad (45)$$

Thus to zero order the escape rate of photons from the unstable circular periodic orbit around the effective extreme black hole of mass M is determined by the leading exponent $\gamma^{(0)} = \lambda = 1/\sqrt{2}M$.

The unique unstable periodic orbit constitutes the repeller. Since the dynamics on this repeller is regular, the Kolmogorov-Sinai entropy is zero, $h_{KS} = \lambda - \gamma^{(0)} = 0$. Thus the system is hyperbolic but nonchaotic. The Pollicott-Ruelle resonances σ_{pr} are given by the zeroes of the Zeta function (28) associated with the single unstable periodic orbit,

$$Z(\sigma_{pr}) = \prod_{k=0}^{\infty} \left(1 - \frac{e^{-\sigma_{pr}T}}{|\Lambda|\Lambda^k} \right)^{k+1} = 0. \quad (46)$$

That is,

$$\sigma_{pr}(k, n) = -\frac{(k+1)}{\sqrt{2}M} + i\frac{n}{M} \quad (47)$$

with $k = 0, 1, 2, \dots$ and $n = 0, \pm 1, \pm 2, \dots$. The resonances belong to the lower half plane of the complex plane σ ($\text{Re } \sigma_{pr} < 0$) and, as occurs in the two-disk scatterer [20, 33], their spectrum forms a semi-infinity periodic array. Here the spacing along the $(\text{Re } \sigma)$ -axis is given by the escape rate $\gamma^{(0)} = 1/\sqrt{2}M$, and by the frequency $w = 2\pi/T = 1/M$ along the $(\text{Im } \sigma)$ -axis. These complex resonances play an important role in the time evolution of an statistical ensemble of photons; they determine the different decay modes and their frequencies in a typical scattering process. The ensemble dynamics is ruled by the resonances which are the closest to the imaginary axis ($k = 0$). The real part of these leading resonances controls the exponential decay on the longest time scale, which defines the escape rate of the system; and their imaginary parts give the frequencies of the oscillations that appear superimposed on the gross exponential decay.

We now study the effect of the angular term in the expansion (38) on the zero-order circular orbit (39) associated with the leading radial term. We still assume the limit $M^2 = (M_1 + M_2)^2 \gg 2M_2d$, in which this term can be treated as an perturbation to the spherically symmetric motion. To make a first order perturbative analysis we write the U^4 function in the interaction term in the form

$$U^4 = \left(1 + \frac{M}{r} \right)^4 + \varepsilon \frac{4M_2d}{r^2} \left(1 + \frac{M}{r} \right)^3 \sin \theta \quad (48)$$

where we have introduced a perturbative parameter ε , which is set equal to one at the end of the analysis. The perturbed trajectory can be written as

$$\begin{aligned} r_1(\xi) &= r_s(\xi) + \varepsilon r_c(\xi) & , & & p_{r1}(\xi) &= p_{rs}(\xi) + \varepsilon p_{rc}(\xi) \\ \theta_1(\xi) &= \theta_s(\xi) + \varepsilon \theta_c(\xi) & , & & p_{\theta 1}(\xi) &= p_{\theta s}(\xi) + \varepsilon p_{\theta c}(\xi) \end{aligned} \quad (49)$$

with first-order corrections to the circular orbit (39) that satisfy the equations of motion

$$r'_c = p_{rc}$$

$$\begin{aligned}
\theta'_c &= \frac{1}{M^2} (p_{\theta c} - 8r_c) \\
p'_{rc} &= -\frac{56M_2d}{M^3} \cos\left(\frac{4}{M}\xi\right) + \frac{8}{M^2} (p_{\theta c} + r_c) \\
p'_{\theta c} &= -\frac{16M_2d}{M^2} \sin\left(\frac{4}{M}\xi\right)
\end{aligned} \tag{50}$$

The periodic solution of this system of equations gives the first-order perturbed orbit,

$$\begin{aligned}
r_1(\xi) &= M + \left[\frac{c}{M^2} + \frac{M_2d}{M^5} \cos\left(\frac{4}{M}\xi\right) \right] \\
\theta_1(\xi) &= \theta_0 + \frac{4}{M}\xi - \left[\frac{9c}{M^4}\xi + \frac{M_2d}{M^6} \sin\left(\frac{4}{M}\xi\right) \right] \\
p_{r1}(\xi) &= -\frac{4M_2d}{M^6} \sin\left(\frac{4}{M}\xi\right) \\
p_{\theta1}(\xi) &= 4M - \left[\frac{c}{M^2} - \frac{4M_2d}{M^5} \cos\left(\frac{4}{M}\xi\right) \right]
\end{aligned} \tag{51}$$

with the constant

$$c = 4M_2Md \left(\frac{1}{M^4} - 1 \right). \tag{52}$$

This is a quasi-circular orbit that nearly reproduces the periodic orbit $\{+-\}$ in two black-hole systems in which $(M_1 + M_2) > d$, and the periodic orbit $\{--\}$ ($\{++\}$) in systems where $(M_1 + M_2) < d$, see figure (6). The more complex periodic orbits (longer symbolic coding) are out of scope of our perturbative analysis. However, in the limit $(M_1 + M_2)^2 \gg 2M_2d$ these are highly unstable periodic orbits that play a secondary role in the escape rate of photons from the black holes. Here the escape rate is controlled by the quasi-circular periodic orbit, $\{+-\}$ or $\{--\}$ ($\{++\}$), that results from the slight deformation of the former photon sphere (an unstable photon orbit) of an effective isolated extreme Reissner-Nordström black hole of mass $M/2$, *i.e.* the circular orbit of radius M . Hence the analysis of the linear stability of the zero- and first-order periodic orbits, (39) and (51), should provide a good estimation of the escape rate of photons from a perturbed black hole. Indeed, as the results in Table (III) indicate, both the analytical escape rate $\gamma^{(0)} = 1/\sqrt{2}M$ derived from the analysis of the linear stability of the zero-order circular orbit (39) and the numerical escape rate $\gamma_{num}^{(1)}$ obtained from the leading eigenvalue of the fundamental matrix of the first-order quasi-circular orbit (51) are close to the escape rate γ_{num} calculated from the numerical simulations with statistical ensembles of photons, see figure (7). As figure (4) shows, the zero-order analytical estimation $\gamma^{(0)} = 1/\sqrt{2}M$ even provides an approximated value for the escape rate from a system of two black holes with similar masses.

In the numerical simulations with statistical ensembles of photons, see figure (7), the escape from the perturbed black hole presents a pronounced oscillation superposed on the gross exponential

System	$\gamma^{(0)}$	$\gamma_{num}^{(1)}$	γ_{num}
$(M_1 = 1, M_2 = 0.01, d = 2)$	0.7001	0.7043	0.6620
$(M_1 = 7, M_2 = 0.1, d = 2)$	0.0996	0.1048	0.0934

TABLE III: Escape rate values for two systems of perturbed black holes. $\gamma^{(0)}$ is the escape rate derived from the zero-order circular orbit (39), $\gamma_{num}^{(1)}$ is the numerical escape rate obtained from the analysis of linear stability of the first-order orbit (51) and γ_{num} is the escape rate calculated from the numerical simulations with statistical ensembles of photons.

decay at the escape rate γ_{num} . The zero-order Pollicott-Ruelle resonances (47) account for this behavior of the decay curves; the exponential decay at the escape rate $\gamma_{num} \simeq \gamma^{(0)} = 1/\sqrt{2}M$ is given by the real part of the leading resonances $k = 0$, and the frequency of the oscillation $w = 2\pi/T \simeq 2\pi M$ is given by the imaginary part of the leading resonance given by $n = 1$ ($k = 0$). This is another indication of the leading role of the quasi-circular orbit that results from the deformation of the former photon sphere of an effective Reissner-Nordström black hole of mass $M/2$ in the escape dynamics of photons.

VIII. CONCLUSIONS

We have studied the scattering of photons in the Majumdar-Papapetrou static spacetime of two extreme Reissner-Nordström black holes held fixed in space due to the balance between the gravitational attraction of their masses and the electrostatic repulsion of their charges. We have identified the set of unstable periodic orbits that constitute the fractal repeller which fully characterizes the chaotic escape dynamics of the photons from the two black holes. These orbits were classified according to a symbolic coding.

The linear stability of the dynamics, in particular the unstable periodic orbits, was analyzed through their stretching factors, which are given by the eigenvalues of the fundamental matrix integrated up to one primitive period of the orbits. With the primitive periods and stretching factors of the periodic orbits we determined the topological pressure, and from this function and its derivative the main quantities of chaos that characterize the fractal repeller associated with the set of unstable periodic orbits were obtained. In particular the escape rate, which was calculated using the trace formulae for hyperbolic flows of Cvitanovic and Eckhardt. This escape rate derived from the periodic orbit theory was in good agreement with the value obtained from numerical simulations that consider the escape dynamics of statistical ensembles of photons.

From the analysis of the linear stability of the dynamics we also identified the periodic orbit that plays the leading role in the escape of photons from the two black-hole configuration. In systems with two identical extreme Reissner-Nordström black holes the escape is mainly controlled by the outermost periodic orbit $\{+-\}$ that encircles the two black holes. In systems where a main black hole of mass M_1 is perturbed by the weak interaction with a black hole of mass M_2 , the escape of photons is dominated by the quasi-circular orbit that results from the slight deformation of the former photon sphere of an effective isolated extreme Reissner-Nordström black hole of mass $M/2 = (M_1 + M_2)/2$, which is a circle of radius M . Depending on the separation distance between the two black holes this leading orbit covers the whole system, and corresponds to the periodic orbit $\{+-\}$, or only encircles the main black hole, and is given by the periodic orbit $\{++\}$ ($\{--\}$).

In systems of a perturbed black hole, the analysis of the linear stability of the unique zero-order periodic orbit in a perturbative treatment provides an analytical estimation for the escape rate, $\gamma^{(0)} = 1/\sqrt{2}M$, which is in good agreement with numerical value derived from the analysis of the linear stability of the first-order perturbative periodic orbit, and also with the escape rate obtained from the time evolution of statistical ensembles of photons. This analytical value even provides an approximated value for the escape rate of photons from a system of two extreme Reissner-Nordström black holes with similar masses.

Acknowledgments

D. Alonso thanks C.P. Dettmann for fruitful discussions. Financial support has been provided by Ministerio de Educación y Ciencia (FIS2004-05687) and Gobierno de Canarias (PI2004/025).

References

-
- [1] See for example D. Hobill, A. Burd, A. Coley (Eds.), *Deterministic Chaos in General Relativity*, (New York: Plenum Press, 1994) and references therein.
 - [2] S. Chandrasekhar, Proc. R. Soc. Lond. **A 421**, 227 (1989).
 - [3] G. Contopoulos, Proc. R. Soc. Lond. **A 431**, 183 (1990); **A 435**, 551 (1991).
 - [4] C.P. Dettmann, N.E. Frankel and N.J. Cornish, Phys. Rev. D **50**, R618, (1994); Fractals **3**, 161 (1995).
 - [5] N.J. Cornish and N.E. Frankel, Phys. Rev. D **56**, 1903 (1997); R. Moeckel, Commun. Math. Phys. **150**, 415 (1992); W. M. Vieira and P. S. Letelier, Phys. Rev. Lett. **76**, 1409 (1996); J. Levin, Phys. Rev. D

- 60**, 064015 (1999); J. Levin **67**, 044013 (2003); N. J. Cornish and J. Levin, *Class. Quantum Grav.* **20**, 1649 (2003).
- [6] L. Bombelli and E. Calzetta, *Class. Quantum Grav.* **9**, 2573 (1992); P.S. Letelier and W.M. Vieira, *Class. Quantum Grav.* **14**, 1249 (1997); N.J. Cornish, *Phys. Rev. D* **64**, 084011 (2001); K. Kiuchi and K. Maeda, *Phys. Rev. D* **70**, 064036 (2004).
- [7] S. Suzuki and K. Maeda, *Phys. Rev. D* **55**, 4848 (1997); S. Suzuki and K. Maeda, *Phys. Rev. D* **61**, 024005 (2000); J. Levin, *Phys. Rev. Lett.* **84**, 3515 (2000); A. Gopakumar and C. Königsdörffer, *Phys. Rev. D* **72**, 121501(R) (2005).
- [8] V. Karas and D. Vokrouhlicky, *Gen. Relativ. Gravit.* **24**, 729 (1992); M. Santoprete and G. Cicogna, *Gen. Rel. Grav.* **34**, 1107 (2002).
- [9] <http://www.ligo.caltech.edu> ; <http://wwwcascina.virgo.infn.it> ; <http://www.geo600.uni-hannover.de> ; <http://tamago.mtk.nao.ac.jp> ; <http://www.gravity.uwa.edu.au/> ; <http://lisa.jpl.nasa.gov>.
- [10] N. J. Cornish and J. Levin, *Phys. Rev. D* **68**, 024004 (2003); J. Levin, R. O'Reilly, and E.J. Copeland, *Phys. Rev. D* **62**, 024023 (2000); A.P.S. Moura and P.S. Letelier, *Phys. Rev. E* **62**, 4784 (2000); D. Hartl and A. Buonanno, *Phys. Rev. D* **71**, 024027 (2005).
- [11] S. D. Majumdar, *Phys. Rev.* **72**, 390 (1947); A. Papapetrou, *Proc. Roy. Irish Acad. A* **51**, 191 (1947).
- [12] U. Yurtsever, *Phys. Rev. D* **52**, 3176 (1995).
- [13] G. Contopoulos and M. Harsoula, *J. Math. Phys.* **45**, 4932 (2004); *Cel. Mech. Dyn. Astron.* **92**, 189 (2005); *Ann. N.Y. Acad. Sci.* **1045**, 139 (2005).
- [14] R. Artuso, E. Aurell and P. Cvitanović. *Nonlinearity* **3**, 325 (1990).
- [15] P. Cvitanović and B. Eckhardt. *J. Phys. A: Math. Gen.* **24**, L237 (1991).
- [16] P. Gaspard and S.A. Rice, *J. Chem. Phys.* **90**, 2225 (1989); **90**, 2242 (1989); **90** 2255 (1989).
- [17] S. Chandrasekhar *The Mathematical Theory of Black Holes*, Oxford University Press, (1983).
- [18] J.B. Hartle and S.W. Hawking, *Commun. Math. Phys.* **26**, 87 (1972).
- [19] V. I. Arnold and A. Avez, *Ergodic Problems of Classical Mechanics*, Benjamin, New York (1968).
- [20] P. Gaspard, *Chaos, Scattering and Statistical Mechanics*, Cambridge University Press (1998), and references therein.
- [21] P. Gaspard, D. Alonso and I. Burghardt, *Adv. Chem. Phys.* **XC**, 105 (1995).
- [22] B.O. Koopman, *Proc. Natl. Acad. Sci. U.S.A.* **17**, 315 (1931).
- [23] J. von Neumann, *Proc. Natl. Acad. Sci. U.S.A.* **18**, 70 (1932).
- [24] M. Pollicot, *Invent. Math.* **81**, 413 (1986); *ibid* **85**, 147 (1986).
- [25] D. Ruelle, *Phys. Rev. Lett.* **56**, 405 (1986).
- [26] I. Isola, *Commun. Math. Phys.* **116**, 343 (1988).
- [27] P. Gaspard and D. Alonso Ramírez, *Phys. Rev. A* **45**, 8383 (1992).
- [28] D. Alonso, D. MacKernan, P. Gaspard and G. Nicolis, *Phys. Rev. E*, **54**, 2474 (1996).
- [29] D. Alonso and P. Gaspard, *Chaos*, **3**, 601 (1993); P. Gaspard, D. Alonso, T. Okuda and K. Nakamura, *Phys. Rev. E*, **50**, 2591 (1994).

- [30] S. Smale, *The Mathematics of Time*, New York: Springer-Verlag, (1980).
- [31] D. Ruelle, *Thermodynamic Formalism*. Reading, Massachusetts: Addison-Wesley (1978).
- [32] J.P. Eckmann and D. Ruelle, Rev. Mod. Phys. **57**, 617 (1985); H. Kantz and P. Grassberger, Physica D **17**, 75 (1985).
- [33] P. Gaspard, in P. Garbaczewski and R. Olkiewicz, Eds., *Dynamics of Dissipation*, Lectures Notes in Physics **597**, (Springer-Verlag, Berlin, 2002) pp. 111-164.

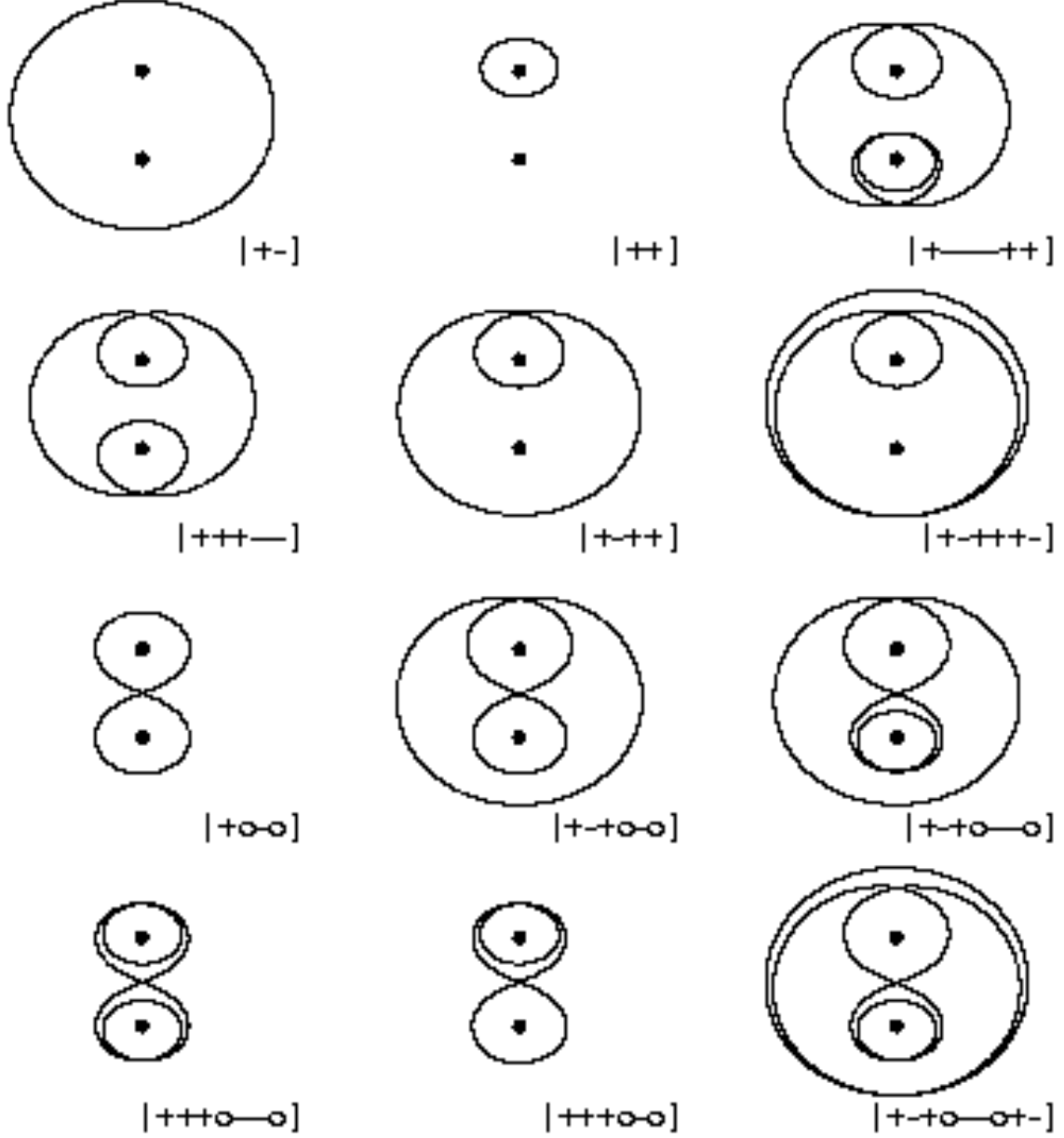


FIG. 1: Set of unstable periodic orbits in a system with two black holes located at $z_{bh} = \pm 1$ and masses $M_1 = M_2 = 1$. The symbolic coding that labels each orbit is indicated. Due to the symmetry of the system with respect to equatorial line (the x -axis), the change of sign of the coordinate z in each orbit on the last two columns gives an additional periodic orbit. The symbolic coding for these *inverse* orbits is obtained exchanging the symbols "+" and "-" in the orbits depicted in these columns. For instance, the inverse orbit of $\{++\}$ has symbolic coding $\{--\}$, the inverse of $\{+ - ++\}$ is $\{- + --\}$, the inverse of $\{+ - + o - o\}$ is $\{- + - o + o\}$ and so on.

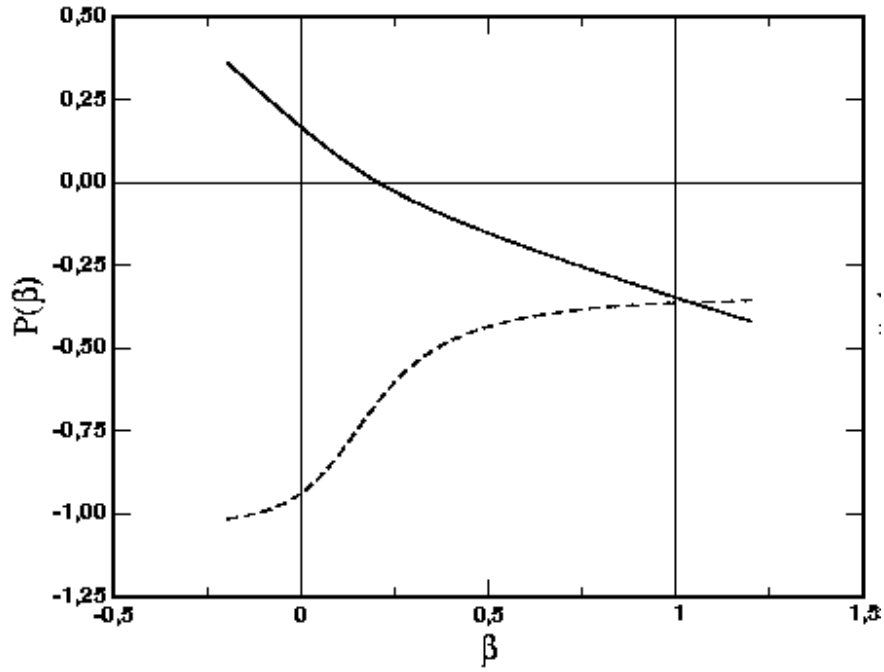


FIG. 2: The solid line gives the pressure function obtained from the three periodic orbits $\{++\}(\{--\})$, $\{+-\}$ and $\{+\circ-\circ\}$, see figure (1). The dashed line is the first derivative of this pressure function.

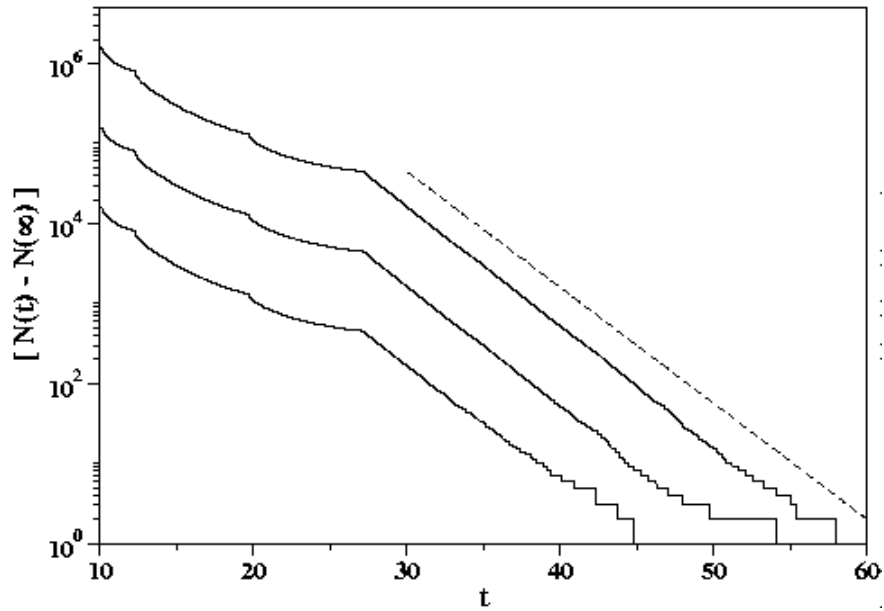


FIG. 3: The evolution with time of $[N(t) - N(\infty)]$ for three ensembles with an increasing number of photons. The dashed line gives the best linear fitting for the ensemble with the highest number of photons.

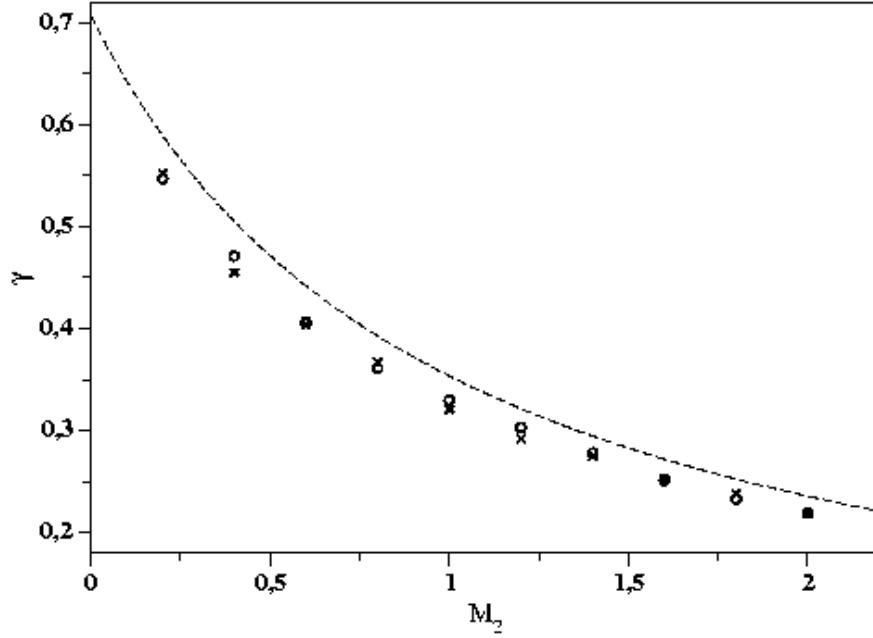


FIG. 4: The escape rate γ from the two black holes located at $z_{bh} = \pm 1$ for different values of the mass M_2 ($M_1 = 1$). The data were obtained considering ensembles of photons with initial velocity parallel to the x-axis and initial positions uniformly distributed along an interval on the z -axis. The circles correspond to an ensemble initially distributed in the interval $[1.1, 4]$ and the crosses to an ensemble initially distributed in the interval $[-4, -1.1]$. The dashed line is the analytical estimation $\gamma^{(0)} = 1/\sqrt{2}(M_1 + M_2)$ for the escape rate from a perturbed black hole, see Section VII.

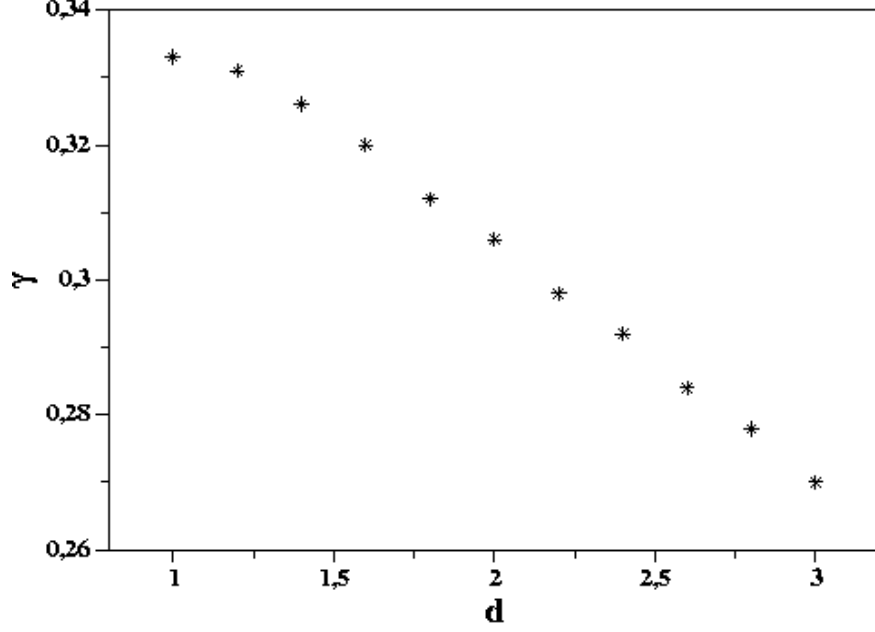


FIG. 5: Escape rate γ from two identical black holes ($M_1 = M_2 = 1$) for different separation distance between them. The black holes are located at $z_{bh} = \pm d$. The data were obtained using ensembles of photons with initial velocity parallel to the x -axis and initial positions uniformly distributed along the z -axis.

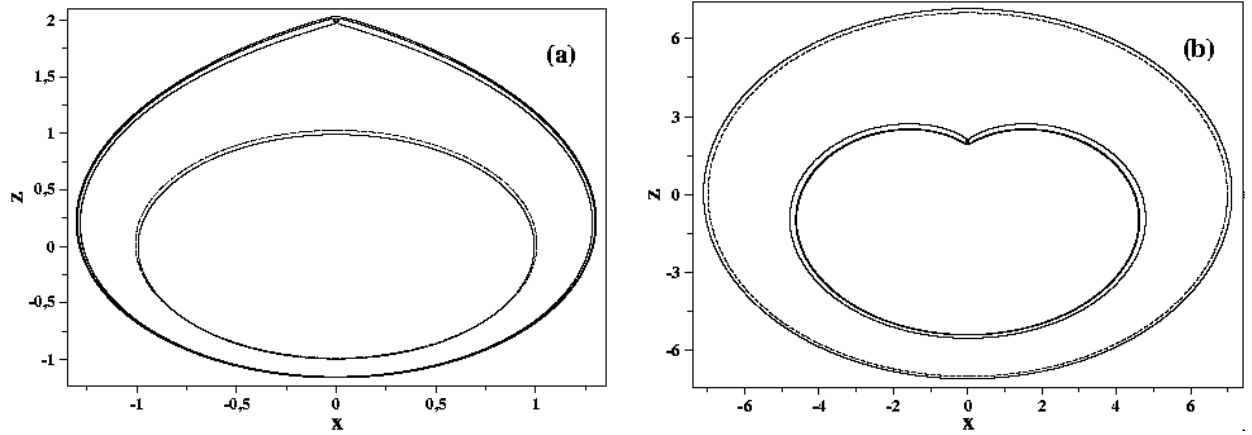


FIG. 6: Some of the periodic orbits in two systems of a black hole of mass M_1 perturbed by the interaction with a black hole of mass M_2 located at distance d . The solid lines give the periodic orbits $\{++\}$, $\{--\}$, $\{+-\}$, $\{+ - ++\}$ and $\{+ \circ - \circ\}$, and the dashed line is the first-order periodic orbit (51). The system (a) corresponds to ($M_1 = 1$, $M_2 = 0.01$, $d = 2$) and (b) to ($M_1 = 7$, $M_2 = 0.1$, $d = 2$). In both systems the main black hole of mass M_1 is located at $(0, 0)$ and the black hole of mass M_2 at $(0, d)$.

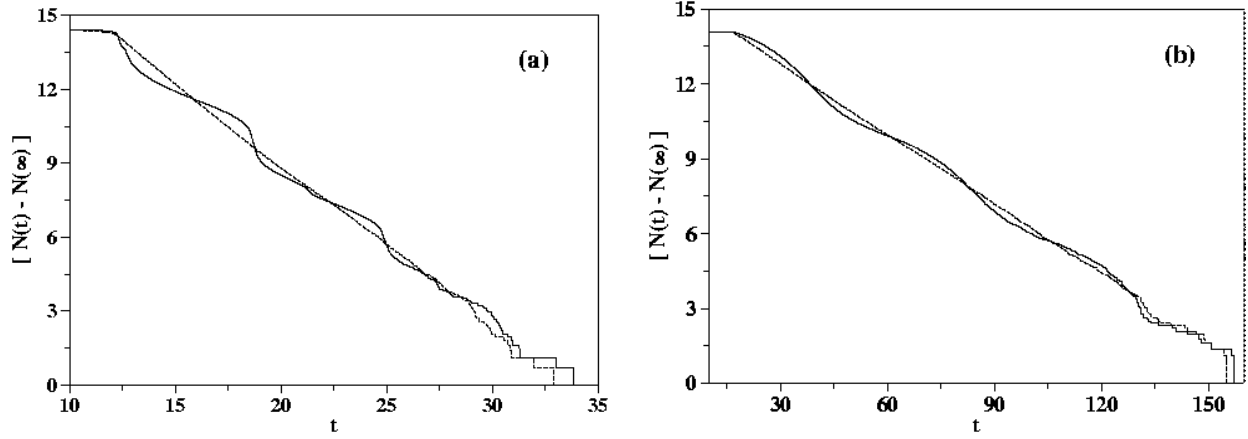


FIG. 7: The evolution with time of $[N(t) - N(\infty)]$ for two statistical ensembles in the perturbed systems (a) and (b) described in figure (6). The solid line gives the escape from a circle of control centered in between the two black holes, at $(0, d/2)$, and the dashed lines the escape from a circle of control centered on the main black hole, at $(0, 0)$. See the Section VII for comments.